Available online at www.sciencedirect.com
ScienceDirect
Journal of Catalysis 254 (2008) 355–364
JOURNAL OF CATALYSIS
www.elsevier.com/locate/jcat

Cobalt- and manganese-substituted ferrites as efficient single-site heterogeneous catalysts for aerobic oxidation of monoterpenic alkenes under solvent-free conditions

Luciano Menini, Márcio C. Pereira, Luciana A. Parreira, José D. Fabris, Elena V. Gusevskaya *

Departamento de Química, Universidade Federal de Minas Gerais, 31270-901, Belo Horizonte, MG, Brazil

Received 3 December 2007; revised 9 January 2008; accepted 12 January 2008

Available online 8 February 2008

Abstract

Cobalt- and manganese-substituted ferrites were used as heterogeneous catalysts for liquid-phase aerobic oxidation of various monoterpenic alkenes. The materials were prepared by co-precipitation and characterized by Mössbauer spectroscopy, powder X-ray diffractometry, magnetization measurements, and elemental analysis. The results show that isomorphic substitution of iron in the ferrite crystalline structure occurred preferentially at octahedral positions and strongly affected its catalytic properties in the oxidation of monoterpenes. Various valuable oxygenated monoterpenic compounds were obtained with high combined selectivities (75–95%) at ca. 40% substrate conversions. Oxidations of β-pinene and 3-carene led almost exclusively to allylic mono-oxygenated derivatives, whereas limonene and α-pinene gave both epoxides and allylic products. The use of inexpensive catalyst and oxidant, solvent-free conditions, and high final product concentrations (ca. 40 wt%) are significant practical advantages of this environmentally friendly process. The catalysts undergo no metal leaching and can be easily recovered by the application of an external magnet and reused.

Keywords: β-Pinene; α-Pinene; Limonene; 3-Carene; Autoxidation; Cobalt catalysts; Manganese catalysts

1. Introduction

The replacement of conventional stoichiometric oxidations, which produce large amounts of hazardous byproducts, by much more benign catalytic processes is a pronounced tendency in the modern fine chemicals industry [1–3]. Economic and environmental advantages of using molecular oxygen as an oxidant are clearly apparent; however, transition metal catalysts are required in these reactions, because uncatalyzed autoxidations usually are nonselective. Thus, the development of selective aerobic oxidations of organic compounds represents a constant goal in catalysis research. Other important challenges for green chemistry are the development of solvent-free technologies to minimize the amount of effluents and the use of solid materials in liquid-phase reactions instead of conventional homogeneous systems to facilitate catalyst recovery.

The conventional heterogenization of homogeneous redox systems on a solid support by impregnation methods for using in liquid-phase oxidations often faces serious leaching problems due to the solubility of active components in a reaction mixture. However, heterogeneous gas-phase oxidations are much more technically demanding; besides, their application in fine chemistry is restricted by limited volatility and thermal stability of complex substrates. Among the most promising approaches to the development of truly heterogeneous catalysts for liquid-phase oxidations is the immobilization of redox-active metals in a solid material by isomorphic substitution in framework positions of molecular sieves and other inorganic matrices [1]. Besides providing greater stability toward leaching, such techniques can result in site isolation of active metal ions in solid matrices, preventing their aggregation to less-reactive species [1]. In some cases, advanced immobilized solid

* Corresponding author. Fax: +553134095700.
E-mail address: elena@ufmg.br (E.V. Gusevskaya).

0021-9517/$ – see front matter
doi:10.1016/j.jcat.2008.01.013

catalysts can show even better catalytic performance than their homogeneous counterparts.

Spinel iron oxides, such as magnetite Fe_3O_4, form an important class of materials for oxidative catalysis because of several features. First, iron can be isomorphously replaced in the magnetite structure by various other transition metals to maintain the spinel framework, which can significantly affect the physicochemical behavior and redox characteristics of the resulting solid [4–8]. Such isomorphic substitutions can be used to tune the catalytic properties of a material. Indeed, it has been reported that incorporation of Co [4–6], Mn [5–7], or Cr [8] in the spinel lattice of magnetite significantly modified its catalytic activity in various reactions. In particular, we recently studied the behavior of iron oxides in the oxidation of β-pinene and observed a remarkable beneficial effect of the partial replacement of Fe by Mn or Co on the catalytic activity of magnetite [5]. The second important benefit from using magnetites and, in general, ferrites as catalysts in liquid-phase reactions is that their magnetic properties provide a convenient route for the catalyst separation from the reaction medium by simple application of an external permanent magnet.

The aim of the present work was to apply Co- and Mn-containing ferrites, in which Co and Mn ions are isolated in inorganic matrices, as heterogeneous "single-site" catalysts for liquid-phase aerobic oxidations of the most abundant natural monoterpenes (i.e., limonene and α-pinene), as well as 3-carene. Oxygenated derivatives of monoterpenes are known to form one of the most important groups of intermediates and ingredients in modern fragrance industry, because they usually demonstrate interesting organoleptic properties [9–11].

For several years, we have been interested in the aerobic oxidation of monoterpenic alkenes catalyzed by palladium [12–14] and cobalt [5,15,16] compounds. Although cobalt-catalyzed autoxidation of alkylbenzenes and alkanes has been studied extensively because of their industrial importance, surprisingly, autoxidation of alkenes has attracted much less attention [17–19]. Several reports on the cobalt-catalyzed homogeneous autoxidation of limonene [15,20], α-pinene [15,20–25], 3-carene [21–23,26], and β-pinene [15,20] have been published. The autoxidation of α-pinene has gained more attention, likely because one of its oxidation products (i.e., verbenone) is used for the synthesis of taxol, an important therapeutic agent. Some cobalt-containing solid materials (e.g., zeolites, silicates, and polyoxometalates) also have been applied as catalysts in the autoxidation of α-pinene and limonene [16,27–29]. Although important advances have been made in the field, the development of more selective and more environmentally friendly catalytic processes for the oxidation of these substrates remains a challenge in fine chemistry.

In the present work, we report simple and efficient aerobic oxidations of various monoterpenes with high combined selectivities for valuable epoxy and/or allylic derivatives under mild solvent-free conditions, in which Co- or Mn-doped ferrites ($Fe_{3-x}M_xO_4$) are used as heterogeneous, low-cost, and readily recyclable catalysts.

2. Experimental

All reagents were purchased from commercial sources and used as received, unless indicated otherwise. Monoterpenes were distilled at reduced pressure and stored in a refrigerator.

2.1. Catalyst preparation and characterization

The ferrites were prepared by co-precipitation of the precursor ferric hydroxyacetate containing cobalt or manganese, followed by thermal treatment for 2 h at 430 °C under a nitrogen atmosphere. The precursor was synthesized from mixed ferric nitrate and cobalt(II) or manganese(II) nitrate solutions by precipitation with concentrated ammonium hydroxide solutions, washed with ammonium acetate, and then dried at 100 °C for 12 h [30]. All prepared ferrites were stored under nitrogen atmosphere to prevent long-term oxidation with air. The ferrites were characterized with powder X-ray diffractometry (XRD) in a Rigaku model Geigerflex equipment using Co($K\alpha$) radiation scanning from 20 to 75° (2θ) at a scan rate of 0.5° min^{-1} and using silicon as an external standard. Diffractrograms of these materials were fitted by the Rietveld method using the software FULLPROF SUITE 2007 (available at http://www-llb.cea.fr/fullweb/winplotr/winplotr.htm) to estimate the structural parameters of the phases obtained. Mössbauer spectra were collected in a constant acceleration transmission mode with a ca. 50-mCi Co^{57}/Rh gamma-ray source. A spectrometer equipped with a transducer (CMTE model MA250) controlled by a linear function-driving unit (CMTE model MR351) was used to obtain the spectra at 25 °C. Mössbauer isomer shifts were quoted relatively to α-Fe. The experimental reflections were fitted to Lorentzian functions with the least squares fitting statistical procedure of the NORMOS^{TM}-90 computer program (written by R.A. Brand, Laboratory of Applied Physics, University of Duisburg, Duisburg, Germany). Magnetization measurements were performed with a portable magnetometer with a fixed magnetic field of ca. 0.3 T calibrated with a nickel metal [31]. Total Fe, Mn, and Co contents were measured by atomic absorption analyses (Carls Zeiss Jena AAS) and Fe^{2+} content was determined by titration with $K_2Cr_2O_7$ in a CO_2 atmosphere to avoid the oxidation of Fe^{2+} to Fe^{3+}. The textural characteristics of the catalysts were determined from nitrogen adsorption isotherms (Autosorb 1; Quantachrome).

2.2. Catalytic oxidation experiments

Reactions were carried out in a glass reactor equipped with a magnetic stirrer and a sampling system and connected to a gas burette to monitor oxygen uptake. Although the catalysts were magnetic materials, the presence of a small magnetic puck in the reaction slurry did not prejudice the reaction because the magnetic field of the puck was weak; thus, virtually all of the catalyst particles became suspended in the solution with stirring. In a typical run, a mixture of monoterpene (18 mmol), dodecane (1 mmol, internal standard) and the catalyst (0.03 g, ca. 1 wt%) was stirred intensively at 60 °C and oxygen pressure of 1 atm for 7 h. Reactions were followed by measuring

the dioxygen uptake and by gas chromatography (GC) using dodecane as an internal standard (Shimadzu model 17, with a Carbowax 20 M capillary column). To take the aliquots for the GC analysis at appropriate time intervals, stirring was stopped and the catalyst was quickly settled by applying the external permanent magnet. The aliquots were diluted 20-fold with acetonitrile before the analysis.

Catalyst recycling experiments were performed as follows: After the reaction, the catalyst was magnetically fixed at the bottom of the reactor; then the solution was taken off with a pipette, and the reactor was recharged with fresh substrate. To control metal leaching, the catalyst was removed at the reaction temperature after 2 h, and the solution was allowed to react further.

The structures of the products **6** and **8–18** were confirmed by GC/MS (Hewlett-Packard MSD 5890/series II, 70 eV) by comparison with authentic samples. Products **5** and **7** were isolated by column chromatography (silica) using mixtures of hexane and CH_2Cl_2 as eluents (**7** was isolated as a mixture with **5**) and identified by GC/MS and NMR (Bruker DRX-400, tetramethylsilane, $CDCl_3$).

3-Carene-5-one (**5**): MS (*m*/*z*/rel.int.): 150/45 (M^+); 135/27 (M^+–CH_3); 109/32; 108/50; 107/95; 105/29; 95/27; 91/100; 80/33; 79/91; 77/57; 67/60; 65/42; 55/33; 53/62; 51/43. ^{1}H NMR, δ_H (*J*, Hz): 1.04 (s, 3H, C^8H_3); 1.19 (s, 3H, C^9H_3); 1.45 (t, 1H, C^1H, $^3J_{1\text{-}6} = {}^3J_{1\text{-}2} = 8.0$); 1.56 (d, 1H, C^6H, $^3J_{6\text{-}1} = 8.0$); 1.87 (s, 3H, $C^{10}H_3$), 2.32 (d, 1H, C^2HH, $^2J = 21.1$); 2.64 (dd, 1H, C^2HH, $^2J = 21.1$, $^3J_{2\text{-}1} = 8.0$); 5.83 (s, 1H, C^4H). ^{13}C NMR, δ_C: 14.38 (C^8); 22.56 (C^7); 23.66 (C^{10}); 25.88 (C^1); 27.87 (C^2); 28.43 (C^9); 32.86 (C^6); 126.42 (C^4); 158.97 (C^3); 196.67 (C^5). Compound described in [32].

2-Carene-4-one (**6**): 150/16 (M^+); 135/9 (M^+–CH_3); 108/80; 107/100; 91/71; 79/66; 77/42; 3/30.

3-Carene-2-one (**7**): 150/6 (M^+); 135/44 (M^+–CH_3); 119/39; 109/100; 95/27; 91/76; 79/34; 77/40; 67/34; 65/37; 55/27. ^{1}H NMR, δ_H (*J*, Hz): 1.10 (s, 3H, C^8H_3); 1.15 (s, 3H, C^9H_3); 1.27–1.32 (m, 1H, C^6H); 1.79 (s, 3H, $C^{10}H_3$), 1.80 (d, 1H, C^1H, $^3J_{1\text{-}6} = 8.2$); 6.66 (t, 1H, C^4H, $^3J_{4\text{-}5} = 6.5$). ^{13}C NMR, δ_C: 138.99 (C^6); 201.65 (C^2).

3-Carene oxide (**8**): 152/1 (M^+); 137/42 (M^+–CH_3); 119/27; 109/92; 95/37; 93/30; 91/36; 81/65; 79/40; 69/28; 68/28; 67/100; 55/49. Compound described in [32].

Trans-pinocarveol (**9**): 152/1 (M^+); 134/15 (M^+–H_2O); 119/26 (M^+–H_2O–CH_3); 92/100; 91/75; 83/52; 70/45; 69/33; 55/91.

Pinocarvone (**10**): 150/13 (M^+); 135/20 (M^+–CH_3); 108/80; 107/55; 91/22; 81/71; 79/30; 69/20; 53/100.

Myrtenal (**11**): 150/1 (M^+); 135/12 (M^+–CH_3); 108/51; 107/100; 106/50; 105/48; 91/45; 79/85; 77/35.

Myrnetol (**12**): 152/1 (M^+); 134/1 (M^+–H_2O); 119/12 (M^+–H_2O–CH_3); 108/40; 96/20; 91/55; 79/100.

Verbenone (**13**): 150/26 (M^+); 135/45 (M^+–CH_3); 107/100; 91/65; 89/40; 79/35; 55/20.

Trans-verbenol (**14**): 152/1 (M^+); 137/9 (M^+–CH_3); 119/20 (M^+–H_2O–CH_3); 109/100; 95/50; 94/71; 91/62; 81/80; 79/59; 77/38; 69/50; 67/62; 59/38; 55/65; 53/47.

α-Pinene oxide (**15**): 152/1 (M^+); 137/20 (M^+–CH_3); 109/47; 95/22; 83/45; 82/34; 81/20; 69/24; 67/100; 55/28.

Trans-carveol (**16**): 134/24 (M^+–H_2O); 119/15 (M^+–H_2O–CH_3); 109/45; 95/23; 91/24; 84/100; 83/36; 69/70; 67/30; 56/36; 55/85; 53/45.

Carvone (**17**): 150/1 (M^+); 135/1 (M^+–CH_3); 108/27; 107/15; 93/27; 91/15; 82/100; 53/30; 54/61.

Limonene oxide (**18**): 152/2 (M^+); 137/35 (M^+–CH_3); 109/47; 108/23; 95/24; 93/50; 82/30; 79/50; 71/30; 67/100; 55/32; 53/36.

3. Results and discussion

3.1. Catalyst characterization

The results of the elemental analysis of the prepared samples (Table 1) show that a chemical composition of the synthesized nondoped material was close to that of a pure magnetite (Fe_3O_4), whereas the Co- and Mn-doped materials (Co–Fe_3O_4 and Mn–Fe_3O_4) contained 13 wt% of the doping metal, corresponding to the approximate formula of $Fe_{2.4}M_{0.5}\otimes_{0.1}O_4$ for both samples (M = Co or Mn; ⊗ = cation vacancy).

The powder XRD (Fig. 1) and room temperature Mössbauer (Fig. 2) analyses indicate the existence of a single crystallographic phase corresponding to magnetite in the nondoped sample (JCPDS card # 1-1111 [33]) and the coexistence of two crystallographic phases corresponding to Co- or Mn-containing spinel ferrites in each doped sample. R_{wp}, R_p, R_B, and R_f parameters obtained from the Rietveld fitting of XRD patterns (Table 2) confirm a good agreement of calculated profiles with the experimental data (Fig. 1). The formation of individual manganese or cobalt oxides was not detected; thus, the incorporation of doping metals seemed to occur through the isomorphic substitution of iron cations in the magnetite crystalline structure. The results of magnetization measurements corroborate this interpretation of the XRD and Mössbauer data; as expected, the isomorphic substitution induced a strong decrease in magnetization values for both Co–Fe_3O_4 and Mn–Fe_3O_4 compared with that of pure Fe_3O_4 (Table 1).

Quantitative analysis of the diffractograms presented in Fig. 1 reveals that Co–Fe_3O_4 and Mn–Fe_3O_4 had broader reflections compared with those of Fe_3O_4. This broadening effect can be related to a smaller size of the ferrite particles. Indeed, estimation of the average crystallite size from the full width at half maximum (obtained from the Rietveld refinement using the Scherrer equation) indicates that the addition of cobalt or manganese induced a significant decrease in particle size for these doped ferrites (Table 2).

Table 1
Elemental analysis and saturation magnetization (σ) data

Sample	Content (wt%)				σ ($J\,T^{-1}\,kg^{-1}$)
	Fe_{total}	Fe^{2+}	Co	Mn	
Fe_3O_4	70	16			85
Co–Fe_3O_4	57	3	13		33
Mn–Fe_3O_4	58	2		13	39

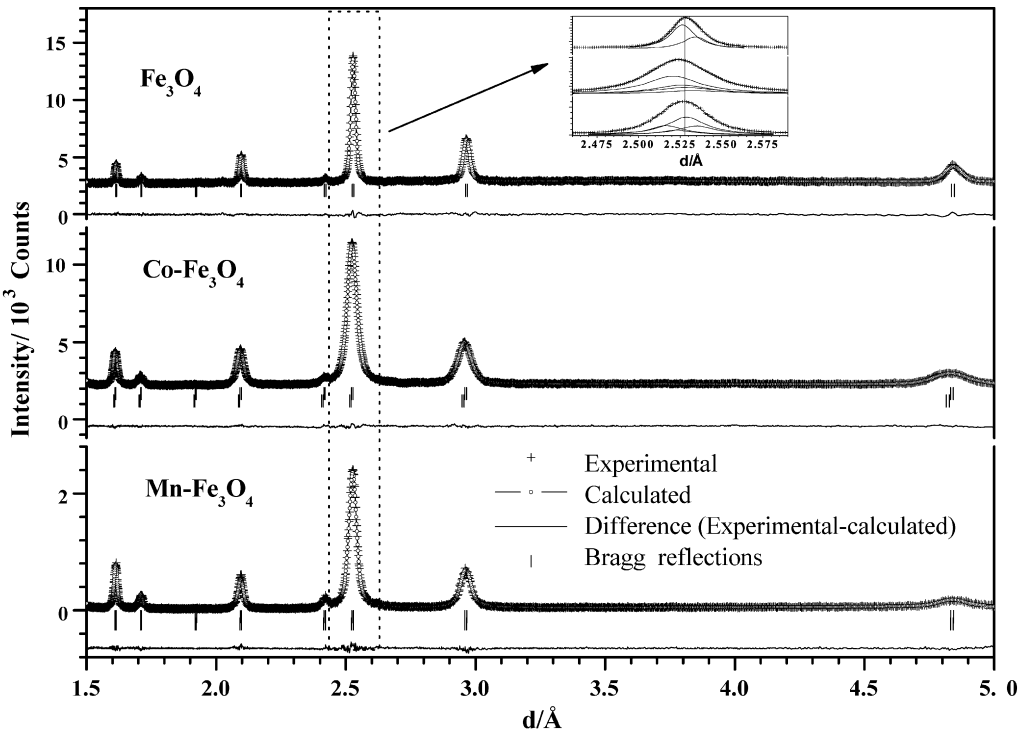

Fig. 1. Powder X-ray diffractograms of the pure magnetite (Fe_3O_4) and Co- (Co–Fe_3O_4) and Mn- (Mn–Fe_3O_4) substituted ferrites fitted by the Rietveld method.

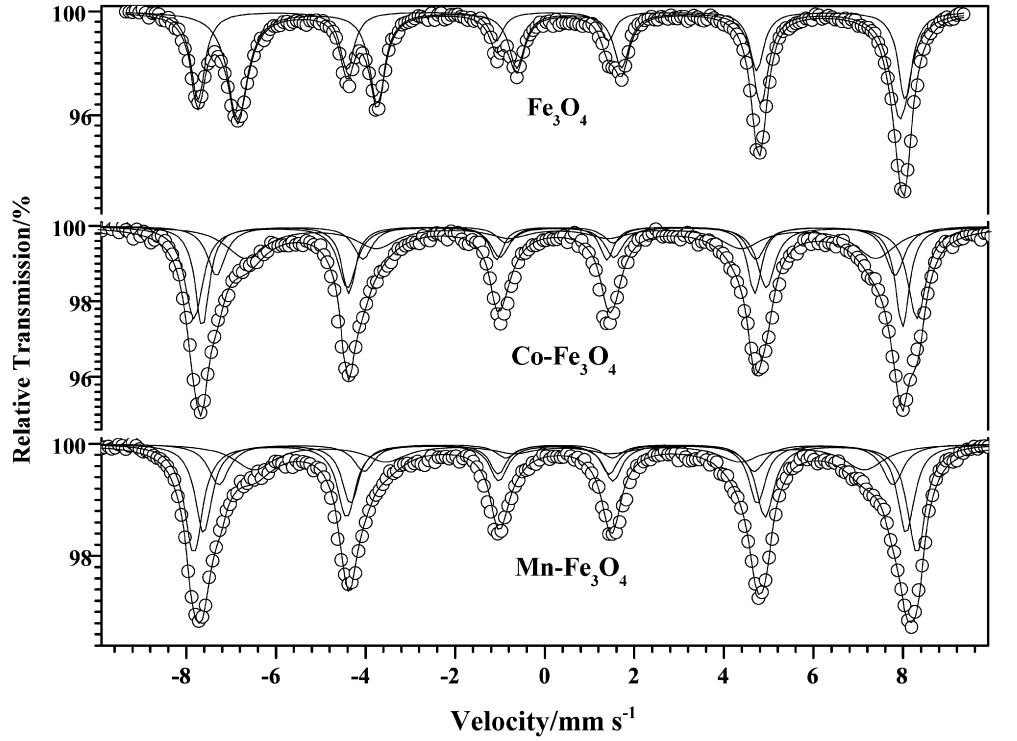

Fig. 2. Room temperature Mössbauer spectra of the pure magnetite (Fe_3O_4) and Co- (Co–Fe_3O_4) and Mn- (Mn–Fe_3O_4) substituted ferrites.

In a stoichiometric magnetite Fe_3O_4, all Fe^{2+} ions typically occupy octahedral positions, whereas Fe^{3+} ions are distributed equally between tetrahedral and octahedral sites. Thus, a typical formula for a stoichiometric magnetite is $[Fe^{3+}]\{Fe^{2+}\ Fe^{3+}\}O_4$, where [ ] and { } denote tetrahedral and octahedral coordination sites, respectively. Fast electron hopping, which is known to be a pair-localized phenomenon in octahedral sites of magnetite, results in $Fe^{2.5+}$ from equal amounts of octahedral Fe^{2+} and Fe^{3+}, yielding the following formula for the material: $[Fe^{3+}]\{Fe_2{}^{2.5+}\}O_4$.

Table 2
Agreement factors for the refinements (R_{wp}, R_p, R_B and R_f)[a], cubic lattice parameters (a_0), chemical formula[b], phase contents and average crystallite sizes of the ferrite particles[c]

Sample	R_{wp}	R_p	R_B	R_f	a_0 (Å)	Chemical formula	Content (wt%)	Crystallite size (nm)
Fe_3O_4	1.79	1.43	6.77	6.57	8.3948	$[Fe]\{Fe_{1.968}\otimes_{0.032}\}O_4$	100	27
Co–Fe_3O_4	5.83	8.50	1.35	1.02	8.3600	$[Fe^{3+}]\{Fe^{3+}_{1.276}Co^{2+}_{0.586}\otimes_{0.138}\}O_4$	59	14
	5.83	8.50	2.13	1.49	8.3858	$[Fe^{3+}]\{Fe^{2+}_{0.296}Fe^{3+}_{1.182}Co^{2+}_{0.431}\otimes_{0.091}\}O_4$	41	15
Mn–Fe_3O_4	12	8.22	3.85	2.99	8.3867	$[Fe^{3+}]\{Fe^{3+}_{1.390}Mn^{2+}_{0.415}\otimes_{0.195}\}O_4$	66	16
	12	8.22	3.33	2.72	8.3900	$[Fe^{3+}]\{Fe^{2+}_{0.241}Fe^{3+}_{1.056}Mn^{2+}_{0.675}\otimes_{0.028}\}O_4$	34	17

[a] Agreement factors were calculated as follows: $R_{wp} = 100[\sum w_i(I_o - I_c)^2 / \sum w_i I_o^2]^{1/2}$; $R_p = 100\sum|I_o - I_c|/\sum I_o$; $R_B = 100\sum|I_{ko} - I_{kc}|/\sum I_{ko}$; $R_f = 100\sum|F_{ko} - F_{kc}|/\sum F_{ko}$; where I_o and I_c—observed and calculated intensities; w_i—weight assigned to each step intensity; I_{ko} and I_{kc}—observed and calculated intensities for Bragg k-reflection; F_{ko} and F_{kc}—observed and calculated structure factors.

[b] Chemical formula were estimated based on the Rietveld refinement of XRD data, Mössbauer and elemental chemical analysis; ⊗—cation vacancy; {} and [] denote tetrahedral and octahedral coordination sites, respectively.

[c] Average crystallite sizes were obtained from XRD data using the Scherrer equation.

Table 3
Mössbauer parameters obtained from the fit of the room temperature spectra of ferrites[a]

Sample	^{57}Fe site	δ (mm s^{-1})	ε (mm s^{-1})	B_{hf} (T)	RA (%)	$R_{B/A}$
Fe_3O_4	A	0.28	−0.01	49.0	36	1.89
	B	0.66	−0.01	45.9	64	
Co–Fe_3O_4	A	0.26	−0.02	48.5	27	1.26
	B	0.38	−0.03	49.9	32	
	A	0.41	−0.08	47.2	17	1.50
	B	0.48	0.02	43.9	24	
Mn–Fe_3O_4	A	0.32	0.02	48.6	28	1.41
	B	0.34	−0.01	50.0	37	
	A	0.39	−0.06	46.7	16	1.26
	B	0.46	−0.08	42.3	19	

[a] A and B—representations for tetrahedral and octahedral coordination sites in the spinel structure, respectively; δ—isomer shift with respect to αFe; ε—quadrupole shift; B_{hf}—magnetic hyperfine field; RA—relative sub-spectral area; $R_{B/A}$—area ratio between octahedral and tetrahedral sites occupancies calculated taking into account that recoilless fractions for octahedral sites are 6% lower than those for tetrahedral sites [35].

The room temperature Mössbauer spectrum for the Fe_3O_4 sample (Fig. 2) confirms the formation of pure magnetite, showing two distinct sextets with typical hyperfine parameters (Table 3), which can be assigned to Fe^{3+} in tetrahedral sites (sites A; $B_{hf} = 49.0$ T; $\delta = 0.28$ mm s^{-1}) and $Fe^{2.5+}$ in octahedral sites (sites B; $B_{hf} = 45.9$ T; $\delta = 0.66$ mm s^{-1}) [34]. The area ratio between octahedral and tetrahedral sites occupancies ($R_{B/A}$) of 1.89 is close to the value expected for pure magnetite ($R_{B/A} = 1.88$). This parameter was calculated taking into account that recoilless fractions for octahedral sites are 6% lower than those for tetrahedral sites [35].

Room temperature Mössbauer spectra for the Co–Fe_3O_4 and Mn–Fe_3O_4 samples can be resolved into four sextets (Fig. 2), two assigned to iron in octahedral sites and the other two assigned to iron in tetrahedral sites of a typical spinel crystal structure. It is generally accepted that the isomer shift is notably higher for iron in octahedral sites [36], and this has been taken as an additional criterion for the assignment of various sextets to their corresponding crystallographic positions. The Mössbauer parameters found for Co–Fe_3O_4 (Table 3) are in agreement with the conclusion that the material contains two main crystallographic phases. The first phase, which apparently has no Fe^{2+} contribution, shows two subspectra, one that could be fitted with a sextet corresponding to tetrahedral A sites ($\delta = 0.26$ mm s^{-1}, $B_{hf} = 48.5$ T) and another that could be fitted with a sextet corresponding to octahedral B sites ($\delta = 0.38$ mm s^{-1}, $B_{hf} = 49.9$ T). Two subspectra of the second crystallographic phase also were fitted with two sextets corresponding to tetrahedral ($\delta = 0.41$ mm s^{-1}, $B_{hf} = 47.2$ T) and octahedral ($\delta = 0.48$ mm s^{-1}, $B_{hf} = 43.9$ T) sites. The increase in the latter isomer shift value may indicate some ferrous character in B sites (i.e., the presence of Fe^{2+} ions in this crystallographic phase) different than the former one. It should be mentioned that the values of hyperfine parameters found for the Co–Fe_3O_4 sample are in agreement with the data reported for ferrites with different Co contents [37,38].

Fitting results for the spectrum of Mn–Fe_3O_4 are similar to those obtained for Co–Fe_3O_4 (Table 3). The Mössbauer parameters found for two crystallographic phases of this Mn-containing ferrite are consistent with the values previously reported for ferrites with different amounts of Mn [39–41].

It is important to note that the area ratios between octahedral and tetrahedral site occupancies for the doped samples were lower than that for pure magnetite (Table 3), indicating that the replacement of Fe by Co and Mn occurred mainly in octahedral sites. Moreover, the decrease in the isomer shifts for octahedral sites in both samples compared with pure magnetite implies that the introduction of Co and Mn decreased the ferrous character of the ferrite; that is, the doping cations preferentially replaced Fe^{2+} ions in the spinel structure.

The powder XRD results are consistent with the Mössbauer and chemical analysis data. The decrease in the cubic lattice parameter (obtained by the Rietveld structural refinement) in the doped samples also confirms the incorporation of Co and Mn into the spinel structure (Table 2). We believe that two factors are responsible for the decrease in lattice parameters of the prepared ferrites: (i) partial oxidation of Fe^{2+} (ionic radium of 78 pm in octahedral coordination) into Fe^{3+} (65 pm) and (ii) isomorphic replacement of Fe^{2+} by Co or Mn. Indeed,

the replacement of Fe^{2+} by either Co or Mn would decrease the lattice dimension (Co^{2+}, −74 pm; Co^{3+}, −61 pm; Mn^{2+}, −82 pm; Mn^{3+}, −65 pm), except in the case of Mn^{2+}, where no significant effect would be expected. On the other hand, the replacement of Fe^{3+} by Co or Mn could not decrease the lattice parameter at all. Thus, the doping cations are more likely to replace mainly the Fe^{2+} ions in octahedral sites of the spinel structure.

Based on the results of our chemical analyses, Mössbauer spectroscopy, and Rietveld refinement of XRD data (occupancy factors for tetrahedral and octahedral crystallographic sites), we estimated the chemical formulas of the prepared ferrites (Table 2). Our BET surface area measurements reveal that all of the catalysts (i.e., Fe_3O_4, Co–Fe_3O_4, and Mn–Fe_3O_4) exhibited adsorption isotherms characteristic of mesoporous materials and showed similar surface areas (31, 43, and 40 $m^2\,g^{-1}$, respectively) and porosity (0.09, 0.15, and 0.14 $cm^3\,g^{-1}$, respectively).

3.2. Catalytic studies

The oxidation of 3-carene (**1**), β-pinene (**2**), α-pinene (**3**), and limonene (**4**) was performed under nonsolvent conditions in the presence of pure magnetite and Co- or Mn-substituted ferrites. In all experiments, these materials alone were applied as catalysts in neat liquid substrates under one atmosphere of molecular oxygen without the addition of bromide ions (which are typically used as auxiliary hydrogen abstraction agents in cobalt-catalyzed oxidation processes). The results, presented in Tables 4–7, show that both the Co- and Mn-containing samples effectively catalyzed the autoxidation of all substrates studied with similar performance, whereas in the presence of pure Fe_3O_4, the conversions were almost as low as those in blank reactions. Selectivities for corresponding products obtained with doped ferrites were the best or among the best reported so far; in some cases, the values were even higher then those reported for homogeneous cobalt catalysts [15]. Each substrate gave only three or four major products with a combined selectivity of 75–95% at ca. 40% conversion, which is a rather high value for reactions most likely involving free radicals. Limonene and α-pinene produced allylic ketones and alcohols as well as epoxides, with a molar ratio of allylic oxidation/epoxidation products of close to 2/1. On the other hand, β-pinene and 3-carene gave allylic mono-oxygenated derivatives almost exclusively.

Because the reactions occur in neat substrates, high concentrations of valuable oxygenated products in final mixtures can be attained (35–40 wt%), which is one of the technological advantages of this method. Although several major products are formed from each substrate, for practical purposes their separation often is not necessary, because the mixtures themselves have interesting organoleptic properties and can be used directly in fragrance compositions. At ca. 40% conversion, the reactions become stagnant, and the catalyst must be separated; however, the catalyst can be reused several times without a significant loss of activity and selectivity (see below). It should be mentioned that adding fresh catalyst to the mixture of the substrate and the products after stagnation of the reaction does not promote additional conversion of the substrate. Thus, it seems that the products accumulated at high concentrations prejudice the reaction, likely acting as radical scavengers.

It is significant that there is no need to remove the catalyst from the reactor; it can be fixed on the glass walls of the reactor using an external hand magnet, after which the solution can be taken off with a pipette and the reactor recharged with fresh substrate. This ease of handling is another attractive feature of our proposed process.

The autoxidation of 3-carene in the presence of Co–Fe_3O_4 occurred smoothly at 60 °C, resulting in a 40% conversion for 7 h (Table 4, run 1). Nearly the same conversion was obtained with half the amount of catalyst (Table 4, run 2), demonstrating that the reaction likely was limited by mass transfer processes. The results of this run corresponded to a turnover number of 206 with respect to the total amount of cobalt in the material; however, the actual efficiency of the surface cobalt species was much higher, because most of the cobalt ions were obviously located in the bulk solid and were not accessible to the substrate. The diffusion limitations seem to be intraparticle ones, because the reaction rate was not affected by changes in the intensity of stirring. On the other hand, with a further decrease in the amount of catalyst (0.3 wt%), the conversion began to decline (Table 4, run 9).

Four major products, all with an intact cyclopropane ring, were identified in the reaction solutions at a combined selectivity of 75% based on the reacted substrate, along with several minor unidentified products. Three allylic ketones—3-carene-5-one (**5**), 2-carene-4-one (**6**), and 3-carene-2-one (**7**)—together accounted for 71% of the mass balance, with 3-carene oxide (**8**) accounting for only 4% (Scheme 1). The molecule of 3-carene contains two double-activated allylic positions, because the activity of the three-membered ring is similar to that of the double bond. As a result, we found good selectivity for α,β-unsaturated ketones, with no corresponding alcohols detected by GC/MS even among the minor products. Almost a half of the substrate was converted into a single product, allylic ketone **5**, reflecting the higher reactivity of the allylic position at carbon 5 versus that at carbon 2. Small amounts of epoxide or epoxide-derived products from 3-carene (which were found in most earlier studies as well) merit special attention. The remarkable selectivity for mono-oxygenated products also should be mentioned; no appreciable amounts of corresponding diketone (3-carene-2,5-dione), which is typically one of the major products in the cobalt-catalyzed oxidation of 3-carene [21,23], were found with the ferrite catalysts.

The cobalt-catalyzed auto-oxidation of 3-carene has been much less widely explored than that of the other monoterpenes studied in the present work. Only a few studies have been reported to date, all of which used homogeneous catalysts and resulted in complex mixtures of mono- and di-oxygenated products, often with opening of the cyclopropane ring [21–23,26]. In previous work [16], we tried to apply sol–gel Co/SiO_2 catalysts for the autoxidation of 3-carene; however, the reaction gave numerous products, including non-GC-determinable oligomers, with low selectivity for any specific compound observed. Although we distilled commercial 3-carene, it was stored at room

Table 4
Oxidation of 3-carene (**1**) catalyzed by ferrites[a]

Run	Catalyst	Conversion (%)	Product selectivity (%)				S_{allyl}[b] (%)	S_{epox}[b] (%)	TON[c]
			Allylic oxidation			Epoxidation			
			5	**6**	**7**	**8**			
1	Co–Fe_3O_4	40	46	14	11	4	71	4	111
2[d]	Co–Fe_3O_4	36	41	16	13	5	70	5	206
3	Mn–Fe_3O_4	30	43	14	10	5	67	5	78
4	Fe_3O_4	4	25	23	8	12	56	12	–
5[e]	Fe_3O_4	4	30	16	10	12	56	12	–
6	None	2	29	18	12	14	59	14	–
7[f]	Co–Fe_3O_4	8	45	15	12	4	72	4	22
8[g]	Co–Fe_3O_4	37	42	16	12	5	70	5	214
9[h]	Co–Fe_3O_4	15	42	15	13	5	70	5	172

[a] Conditions: catalyst (1.2 wt%), 60 °C, 1 atm (O_2), reaction time 7 h. Conversion and selectivity were determined by GC.
[b] Selectivities for allylic oxidation and epoxidation products: **5** + **6** + **7** and **8**, respectively.
[c] TON—moles of the substrate converted/moles of Co or Mn.
[d] 0.6 wt% of the catalyst was used.
[e] The catalyst was treated with H_2 for 2 h at 250 °C before use.
[f] The catalyst was removed by filtration after 2 h at the reaction temperature and the filtrate was allowed to react further.
[g] The catalyst was re-used after run 2; total TON for two reaction cycles is given.
[h] 0.3 wt% of the catalyst was used.

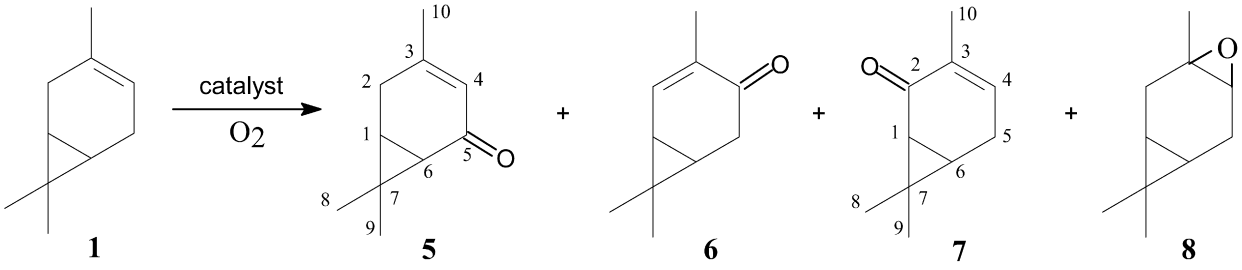

Scheme 1. Oxidation of 3-carene.

temperature under air for several weeks, as were other monoterpenes. It seems that considerable accumulation of peroxidic compounds occurs under such conditions, so that heating such a substrate to 60 °C promotes relatively rapid nonselective transformation even in the absence of cobalt catalysts. In the present work, we used freshly distilled 3-carene and stored it under refrigeration, which allowed us to realize a much more selective catalytic oxidation of this substrate.

The Mn–Fe_3O_4 material also efficiently catalyzed the oxidation of 3-carene (Table 4, run 3). The product composition was very similar to that obtained with Co–Fe_3O_4, even though the reaction was slightly slower and resulted in lower conversion in the same time period (30% vs 40% in 7 h; cf. runs 1 and 3, Table 4). On the other hand, the Fe_3O_4 sample converted only 4% of the 3-carene under similar conditions, and the reaction was much less selective for ketone **5** (Table 4, run 4 vs run 1). Treating the Fe_3O_4 with H_2 at 250 °C before the reaction, with the aim of reducing Fe^{3+} to Fe^{2+}, did not increase the activity of the material (Table 4, run 5). These results confirm once again a remarkable effect of the partial replacement of Fe by Mn or Co in the magnetite on its catalytic activity. It should be mentioned that in blank reactions with no catalyst added, neat 3-carene (as well as limonene, α-pinene, and β-pinene) demonstrated virtually no reactivity (ca. 2% conversion for 7 h at 60 °C; Table 4, run 6).

To control leaching of the active metal, the catalyst was filtered off at the reaction temperature after 2 h of use, and the filtrate was allowed to react further (Table 4, run 7). No additional conversion of 3-carene was observed after the catalyst was removed, supporting heterogeneous catalysis; that is, the reaction solution contained no significant amounts of dissolved cobalt species, and cobalt ions immobilized in the solid matrix were responsible for the oxidation of the substrate. In run 1 after the reaction, the catalyst was magnetically fixed at the bottom of the reactor, and the solution was taken off with a pipette. The spent catalyst with fresh substrate exhibited similar behavior to that in the original reaction (Table 4, cf. runs 1 and 8). Thus, the catalyst released no cobalt to the medium and could be easily recovered either magnetically or by filtration and reused.

For comparison purposes, we studied the reactivity of β-pinene with substituted ferrites prepared in the present work, which are different from the materials used in [5]. The reaction over Co–Fe_3O_4 gave allylic oxidation products almost exclusively (Table 5, run 1). A high combined selectivity of up to 95% for *trans*-pinocarveol (**9**), pinocarvone (**10**), myrtenal (**11**), and myrtenol (**12**) was achieved at a 37% conversion, with each of these products formed in nearly the same amount (Scheme 2). No epoxide or epoxide-derived products were detected in the reaction mixtures. In our previous studies [15,16], β-pinene also exhibited a strong preference for allylic oxidation

Table 5
Oxidation of β-pinene (**2**) catalyzed by ferrites[a]

Run	Catalyst	Conversion (%)	Product selectivity (%)				S_{allyl}[b] (%)	TON[c]
			9	**10**	**11**	**12**		
1	Co–Fe_3O_4	37	25	26	20	24	95	103
2	Mn–Fe_3O_4	30	25	25	21	23	94	78
3	Fe_3O_4	4	23	26	19	22	90	–

[a] Conditions: catalyst (1.2 wt%), 60 °C, 1 atm (O_2), reaction time 7 h. Conversion and selectivity were determined by GC.
[b] Selectivities for allylic oxidation products **9**–**12**.
[c] TON—moles of the substrate converted/moles of Co or Mn.

Table 6
Oxidation of α-pinene (**3**) catalyzed by ferrites[a]

Run	Catalyst	Conversion (%)	Product selectivity (%)			S_{allyl}[b] (%)	S_{epox}[b] (%)	TON[c]
			Allylic oxidation		Epoxidation			
			13	**14**	**15**			
1	Co–Fe_3O_4	36	40	24	26	64	26	100
2	Mn–Fe_3O_4	32	37	23	28	60	28	83
3	Fe_3O_4	5	40	20	10	60	10	–

[a] Conditions: catalyst (1.2 wt%), 60 °C, 1 atm (O_2), reaction time 7 h. Conversion and selectivity were determined by GC.
[b] Selectivities for allylic oxidation and epoxidation products: **13** + **14** and **15**, respectively.
[c] TON—moles of the substrate converted/moles of Co or Mn.

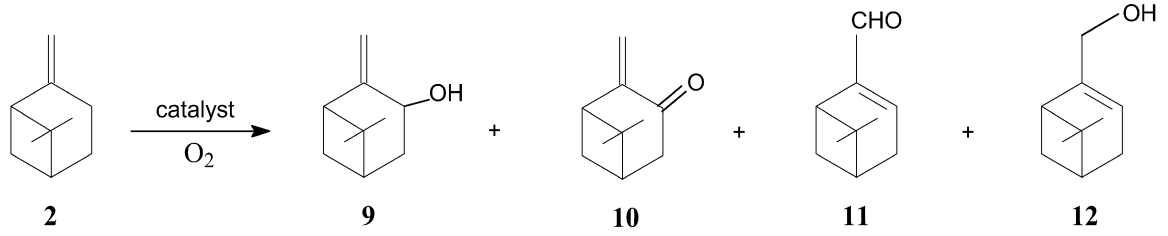

Scheme 2. Oxidation of β-pinene.

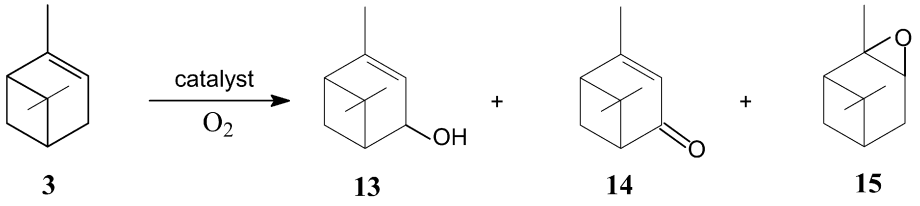

Scheme 3. Oxidation of α-pinene.

over epoxidation. It should be mentioned that selectivities for allylic products obtained with ferrites are even higher than those reported for homogeneous $CoCl_2$/acetonitrile systems [15] and heterogeneous sol–gel Co/SiO_2 catalysts [16]. The Mn–Fe_3O_4 catalyst showed similar conversion and selectivity as Co–Fe_3O_4 (Table 5, run 2 vs run 1).

The oxidation of α-pinene catalyzed by either Co–Fe_3O_4 or Mn–Fe_3O_4 resulted mainly in verbenone (**13**) (ca. 40%), *trans*-verbenol (**14**) (ca. 25%), and α-pinene oxide (**15**) (ca. 25%) with a high combined selectivity of ca. 90% (Scheme 3, Table 6). For both catalysts, a substrate conversion of near 35% was achieved at 60 °C for 7 h.

Limonene also formed three main products: carveol (**16**) (ca. 80% *cis*), carvone (**17**), and limonene oxide (**18**) (*cis*/*trans* ≈ 1/1), each at 20–30% selectivity (Scheme 4, Table 7). Approximately 40% conversion was attained at 60 °C for 7 h with both Co–Fe_3O_4 and Mn–Fe_3O_4. The *endo* cyclic double bond of limonene was much more sensitive to epoxidation; the epoxide resulting from the oxidation of the *exo* cyclic double bond (not shown) was ¼ the amount of epoxide **18** detected.

It is known that in the oxidation of cyclic alkenes, allylic oxidation and epoxidation are often competitive processes and often occur simultaneously [42]. The contribution of each reaction strongly depends on the substrate nature and relative stability of the corresponding intermediates. In cobalt- and manganese-catalyzed homogeneous oxidations of alkenes, a free-radical chain mechanism is usually suggested, and competition between the abstraction of the allylic hydrogen to give allylic oxidation products and the addition of the alkylperoxy radical to the double bond resulting in epoxide products is ex-

Table 7
Oxidation of limonene (**4**) catalyzed by ferrites[a]

Run	Catalyst	Conversion (%)	Product selectivity (%)			S_{allyl}[c] (%)	S_{epox}[c] (%)	TON[d]
			Allylic oxidation		Epoxidation[b]			
			16	**17**				
1	Co–Fe_3O_4	40	25	22	34	47	34	111
2	Mn–Fe_3O_4	38	26	22	33	48	33	98
3	Fe_3O_4	6	28	19	35	47	35	–

[a] Conditions: catalyst (1.2 wt%), 60 °C, 1 atm (O_2), reaction time 7 h. Conversion and selectivity were determined by GC.
[b] Mainly *endo* epoxide **18**, along with small amounts of *exo* epoxide (not shown); *endo*/*exo* ≈ 4/1.
[c] Selectivities for allylic oxidation and epoxidation products: **16** + **17** and **18** + *exo* epoxide, respectively.
[d] TON—moles of the substrate converted/moles of Co or Mn.

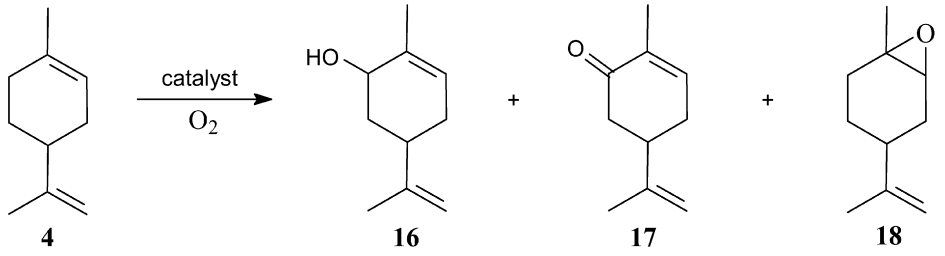

Scheme 4. Oxidation of limonene.

pected [17]. Although the substrates studied in this work are all structural isomers and some of them are often appear together in natural products, these compounds showed different behavior under oxidation conditions. The strong preference exhibited by 3-carene and β-pinene compared with α-pinene and limonene for allylic oxidation over epoxidation can be explained by different reactivity of allylic hydrogens in these molecules toward the abstraction.

It has been suggested that a flexibility of the six-membered ring in 3-carene [23] and a preference of β-pinene to adopt a pseudochair conformation [15] allow some allylic hydrogens in these molecules to assume positions orthogonal to the double bonds. In such arrangements, the abstraction of these hydrogens is promoted by overlapping between the olefinic π-orbital and the developing p-orbital containing an unpaired electron in the transition state. In other words, a so-called "cyclic activation" (i.e., enhanced reactivity of cyclic allylic hydrogens compared to acyclic ones due to the initial arrangement of the molecule similar to the transition state in the course of the hydrogen abstraction [23]) is particularly successful in the β-pinene and 3-carene molecules. Favorability toward the π–p interaction structures of allylic radicals formed from β-pinene and 3-carene makes the allylic oxidation a major reaction. In addition, the allylic route in the oxidation of 3-carene is strongly favored by the stabilization of both allylic radicals (at C_2 and C_5) due to conjugation not only with the double bond, but also with the cyclopropane ring.

4. Conclusion

We have developed an efficient and environmentally friendly catalytic process for the oxidation of monoterpenic alkenes under mild aerobic conditions. The use of inexpensive cobalt- or manganese-containing ferrites as heterogeneous catalysts, molecular oxygen as a final oxidant, and solvent-free conditions are significant practical advantages of this process. The catalysts undergo no metal leaching; they can be readily recovered by simple application of an external permanent magnet and reused several times. This simple and low-cost method provides an attractive entry to the synthesis of high-priced low-volume oxygenated monoterpenes with a remarkable atom economy and high combined selectivity at relatively high substrate conversions. Further studies are targeted toward developing selective aerobic oxidations of other substrates using doped ferrites as catalysts.

Acknowledgments

Financial support from the CNPq and FAPEMIG (Brazil) is gratefully acknowledged. The authors thank Joyce Cristina da Cruz Santos for experimental assistance.

References

[1] I.W.C.E. Arends, R.A. Sheldon, Appl. Catal. A 212 (2001) 175.
[2] R.A. Sheldon, R.S. Downing, Appl. Catal. A 189 (1999) 163.
[3] J.S. Rafelt, J.H. Clark, Catal. Today 57 (2000) 33.
[4] C.G. Ramankutty, S. Sugunan, B. Thomas, J. Mol. Catal. 187 (2002) 105.
[5] L. Menini, M.J. da Silva, M.F.F. Lelis, J.D. Fabris, R.M. Lago, E.V. Gusevskaya, Appl. Catal. A 269 (2004) 117.
[6] R.C.C. Costa, M.F.F. Lelis, L.C.A. Oliveira, J.D. Fabris, J.D. Ardisson, R.V.A. Rios, C.N. Silva, R.M. Lago, J. Hazard. Mater. 129 (2006) 171.
[7] L.C.A. Oliveira, J.D. Fabris, R.R.V.A. Rios, W.N. Mussel, R.M. Lago, Appl. Catal. A 259 (2004) 253.
[8] F. Magalhães, M.C. Pereira, S.E.C. Botrel, J.D. Fabris, W.A. Macedo, R. Mendonça, R.M. Lago, L.C.A. Oliveira, Appl. Catal. A 332 (2007) 115.
[9] W.E. Erman, Chemistry of the Monoterpenes. An Encyclopedic Handbook, Marcel Dekker, New York, 1985, p. 12.
[10] J.L.F. Monteiro, C.O. Veloso, Top. Catal. 27 (2004) 169.
[11] H. Mimoun, Chimia 50 (1996) 620.

[12] M.G. Speziali, P.A. Robles-Dutenhefner, E.V. Gusevskaya, Organometallics 26 (2007) 4003.
[13] M.J. da Silva, J.A. Gonçalves, O.W. Howarth, R.B. Alves, E.V. Gusevskaya, J. Organomet. Chem. 689 (2004) 302.
[14] J.A. Gonçalves, E.V. Gusevskaya, Appl. Catal. A 258 (2004) 93.
[15] M.J. da Silva, P.A. Robles-Dutenhefner, L. Menini, E.V. Gusevskaya, J. Mol. Catal. A 201 (2003) 71.
[16] P.A. Robles-Dutenhefner, M.J. da Silva, L.S. Sales, E.M.B. Sousa, E.V. Gusevskaya, J. Mol. Catal. A 217 (2004) 139.
[17] R.A. Sheldon, J.K. Kochi, Metal-Catalyzed Oxidations of Organic Compounds, Academic Press, London, 1981, p. 133.
[18] G.W. Parshall, S.D. Ittel, Homogeneous Catalysis. The Applications and Chemistry of Catalysis by Soluble Transition Metal Complexes, Wiley, New York, 1992, p. 236.
[19] R.W. Fischer, F. Rohrscheid, in: B. Cornils, W.A. Herrmann (Eds.), Applied Homogeneous Catalysis with Organometallic Compounds, VCH, Weinheim, 1996, p. 439.
[20] M.F.T. Gomes, O.A.C. Antunes, J. Mol. Catal. A 121 (1997) 145.
[21] S.C. Sethi, A.D. Natu, M.S. Wadia, Ind. J. Chem. 25B (1986) 248.
[22] D. Mukesh, S. Bhaduri, V. Khanwalkar, Chem. Eng. J. 41 (1989) 67.
[23] G. Rothenberg, Y. Yatziv, Y. Sasson, Tetrahedron 54 (1998) 593.
[24] M.K. Lajunen, M. Myllykoski, A. Asikkala, J. Mol. Catal. A 198 (2003) 223.
[25] R. Chakrabarty, B.K. Das, J. Mol. Catal. A 223 (2004) 39.
[26] D.A. Baines, W. Cocker, J. Chem. Soc. Perkin Trans. 22 (1975) 2232.
[27] T. Joseph, D.P. Sawant, C.S. Gopinath, S.B. Halligudi, J. Mol. Catal. A 184 (2002) 289.
[28] N.V. Maksimchuk, M.S. Melgunov, Yu.A. Chesalov, J. Mrowiec-Bialon, A.B. Jarzebski, O.A. Kholdeeva, J. Catal. 246 (2007) 241.
[29] N.K. Kala Raj, V.G. Puranik, G. Gopinathan, A.V. Ramaswamy, Appl. Catal. A 256 (2003) 265.
[30] P.P. Abreu Filho, E.A. Pinheiro, F. Galembeck, React. Sol. 3 (1987) 241.
[31] J.M.D. Coey, O. Cugat, J. McCauley, J.D. Fabris, Rev. Fis. Apl. Instrum. 7 (1992) 25.
[32] R.R.L. Martins, M.G.P.M.S. Neves, A.G.D. Silvestre, M.M.Q. Simões, A.M.S. Silva, A.C. Tomé, J.A.S. Cavaleiro, P. Tagliatesta, C. Crestini, J. Mol. Catal. A 172 (2001) 33.
[33] Joint Committee on Powder Diffraction Standards (JCPDS), Mineral powder diffraction files data book, International Center for Diffraction Data, Swarthmore, PA, 1980, p. 1168.
[34] R.E. Vandenbergue, C.A. Barrero, G.M. da Costa, E. van San, E. de Grave, Hyperfine Interact. 126 (2000) 247.
[35] G.A. Sawatzky, F. van der Woude, A.H. Morrish, Phys. Rev. 183 (1969) 383.
[36] J.L. Dormann, J.L. Greneche, G. Pourroy, S. Lakamp, Hyperfine Interact. 112 (1998) 93.
[37] M. Veverka, P. Veverka, O. Kaman, A. Lancok, K. Záveta, E. Pollert, K. Knizek, J. Bohacek, M. Benes, P. Kaspar, E. Duguet, S. Vasseur, Nanotechnology 18 (2007) 1.
[38] M.D.J. Sebastian, B. Rudraswamy, M.C. Radhakrishna, Ramani, Bull. Mater. Sci. 26 (2003) 509.
[39] Y. Li, J. Jiang, J. Zhao, Mater. Chem. Phys. 87 (2004) 91.
[40] M.A. Gabal, S.S. Ata-Allah, J. Phys. Chem. Solids 65 (2004) 995.
[41] J.V. Bellini, S.N. de Medeiros, A.L.L. Ponzoni, F.R. Longen, M.A.C. de Melo, A. Paesano Jr., Mater. Chem. Phys. 105 (2007) 92.
[42] E.F. Murphy, T. Mallat, A. Baiker, Catal. Today 57 (2000) 115.